AVO principles, processing and inversion

Hong Feng and John C. Bancroft

ABSTRACT

In this paper, we will review the basic principles of AVO and introduce some amplitude preserving algorithms. Seismic data processing sequences for AVO analysis and some algorithms for AVO inversion will be discussed. Topics related to AVO, such as rock physics, AVO modeling, AVO interpretation, and AVO pitfalls are beyond the scope of this report.

INTRODUCTION

The AVO (amplitude variation with offset) technique assesses variations in seismic reflection amplitude with changes in distance between shot points and receivers. AVO analysis allows geophysicists to better assess reservoir rock properties, including porosity, density, lithology and fluid content.

Around 1900, Knott and Zoeppritz developed the theoretical work necessary for AVO theory (Knott, 1899; Zoeppritz, 1919), given the P-wave and S-wave velocities along with the densities of the two bounding media. They developed equations for plane-wave reflection amplitudes as a function of incident angle. Bortfeld (1961) simplified Zoeppritz's equation, making it easier to understand how reflection amplitudes depend on incident angle and physical parameters. Koefoed (1955) described the relationship of AVO to change in Poisson's ratio across a boundary. Koefoed's results were based on the exact Zoeppritz equation. The conclusions drawn by Koefoed are the basis of today's AVO interpretation.

Rosa (1976) and Shuey (1985) did breakthrough work related to predicting lithology from AVO, inspired by Koefoed's article. Ostrander (1982) illustrated the interpretation benefits of AVO with field data, accelerating the second era of amplitude interpretation. Allen and Peddy (1993) collected seismic data, well information, and interpretation from the Gulf Coast of Texas and published a practical look at AVO that documented not only successes but also the interpretational pitfalls learned from dry holes.

Today, AVO analysis is widely used in hydrocarbon detection, lithology identification, and fluid parameter analysis, due to the fact that seismic amplitudes at layer boundaries are affected by the variations of the physical properties just above and below the boundaries. In recent years, a growing number of theories and techniques in seismic data acquisition, processing, and seismic data interpretation have been developed, updated, and employed. AVO analysis in theory and practice is becoming increasingly attractive.

PRINCIPLES OF AVO

When seismic waves travel into the earth and encounter layer boundaries with velocity and density contrasts, the energy of the incident wave is partitioned at each boundary.

Specifically, part of the incident energy associated with a compressional source is mode-converted to a shear wave; then both the compressional and shear wave energy are partly reflected from and partly transmitted through each of these layer boundaries.

The fraction of the incident energy that is reflected depends upon the angle of incidence. Analysis of reflection amplitudes as a function of incidence angle can sometimes be used to detect lateral changes in elastic properties of reservoir rocks, such as the change in Poisson's ratio. This may then suggest a change in the ratio of P wave velocity to S wave velocity, which in turn may imply a change in fluid saturation within the reservoir rocks.

Starting with the equations of motion and Hooke's law, one can derive and solve the wave equations for plane elastic waves in isotropic media. Then, using the equations of continuity for the vertical and tangential components of stress and strain at a layer boundary, plane wave solutions and Snell's law that relates propagation angles to wave velocities, one obtains the equation for computing the amplitudes of the reflected and transmitted P- and S- wave. Figure 1 illustrates the wave propagation of incidence of compressible wave at solid-solid interface.

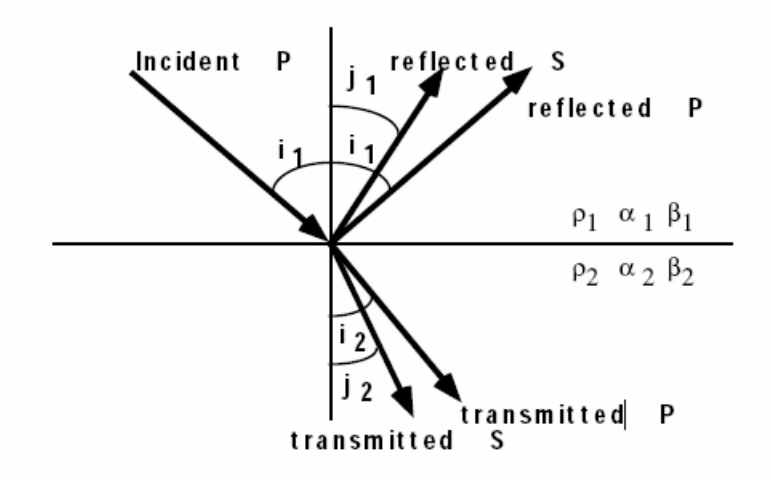

FIG. 1. Waves generated at an interface by an incident P-wave.

Approximations of the Zoeppritz Equations

The Bortfeld Approximation

The Zoeppritz equations allow us to derive the exact plane wave amplitudes of a reflected P wave as a function of angle, but do not give us an intuitive understanding of how these amplitudes relate to the various physical parameters. Over the years, a number of approximations to the Zoeppritz equations have been made. The first was by Bortfeld in 1961. His approximation to the Zoeppritz equation for PP reflection amplitude is given by

$$R(\theta) = \frac{1}{2}\ln\left(\frac{\alpha_2\rho_2\cos\theta_2}{\alpha_1\rho_1\cos\theta_1}\right) + \left[2 + \frac{\ln\frac{\rho_2}{\rho_1}}{\ln\frac{\alpha_2}{\alpha_1} - \ln\frac{\alpha_2\beta_1}{\alpha_1\beta_2}}\right]\frac{\beta_1^{\,2} - \beta_2^{\,2}}{\alpha_1^{\,2}}\sin^2\theta\,. \qquad (1)$$

An important aspect of Bortfeld's equations is that they provide the interpreter with an insight into the amplitude variation with offset as a function of rock properties. The first term in Bortfeld's PP equation is fluid-fluid reflection coefficient. The second term has been called the rigidity term because of its dependence on the S-wave velocity, and thus on the shear rigidity modulus. However, equation (1) does not explicitly indicate angle- or offset- dependence of reflection amplitudes; therefore, its practical implementation for AVO analysis has not been considered.

The Aki, Richards and Frasier Approximation

The Bortfeld approximation was further refined by Richards and Frasier (1976) and by Aki and Richards (1980). The Aki, Richards and Frasier approximation is appealing because it is written as three terms, the first involving P-wave velocity, the second involving density, and the third involving S-wave velocity. Their formula can be written:

$$R(\theta) = a\frac{\Delta\alpha}{\alpha} + b\frac{\Delta\rho}{\rho} + c\frac{\Delta\beta}{\beta}, \qquad (2)$$

where $a = 1/(2\cos^2\theta) = (1+\tan^2\theta)/2$, $b = 0.5 - [(2\beta^2/\alpha^2)\sin^2\theta]$,
$c = -(4\beta^2/\alpha^2\sin^2\theta)$, $\alpha = (\alpha_1+\alpha_2)/2$, $\beta = (\beta_1+\beta_2)/2$, $\rho = (\rho_1+\rho_2)/2$,
$\Delta\alpha = \alpha_2 - \alpha_1$, $\Delta\beta = \beta_2 - \beta_1$, $\Delta\rho = \rho_2 - \rho_1$, $\theta = (\theta_i + \theta_t)/2$, and
$\theta_t = \arcsin[(\alpha_2/\alpha_1)\sin\theta_i]$.

In practice, one does not observe the separate effects of P wave reflectivity $\Delta\alpha/\alpha$, S wave reflectivity $\Delta\beta/\beta$ and fractional change in density $\Delta\rho/\rho$ on the reflection amplitude $R(\theta)$. Instead, one observes changes in reflection amplitude as a function of angle of incidence. Equation (2) can be rearranged in successive ranges of angle of incidence as

$$\begin{aligned} R(\theta) = {} & [\frac{1}{2}(\frac{\Delta\alpha}{\alpha} + \frac{\Delta\rho}{\rho})] + [\frac{1}{2}\frac{\Delta\alpha}{\alpha} - 4\frac{\beta^2}{\alpha^2}\frac{\Delta\beta}{\beta} - 2\frac{\beta^2}{\alpha^2}\frac{\Delta\rho}{\rho}]\sin^2\theta \\ & + [\frac{1}{2}\frac{\Delta\alpha}{\alpha}](\tan^2\theta - \sin^2\theta) \end{aligned} \qquad (3)$$

Equation (3) contains three terms. It was rearranged by Shuey (1985) in terms of Poisson's ratio rather than S wave velocity to give his well known approximation, and was also rearranged by Wiggins (1987) at Mobil, and published by Gelfand and Larner (1986) as an approximation based on S and P wave reflectivity.

Setting the S wave to P wave velocity ratio, $\beta/\alpha = 0.5$, then ignoring the third term in equation (3),

$$R(\theta) = [\frac{1}{2}(\frac{\Delta\alpha}{\alpha} + \frac{\Delta\rho}{\rho})] + [\frac{1}{2}\frac{\Delta\alpha}{\alpha} - \frac{\Delta\beta}{\beta} - \frac{1}{2}\frac{\Delta\rho}{\rho}]\sin^2\theta . \quad (4)$$

Letting

$$R_p \cong \frac{1}{2}(\frac{\Delta\alpha}{\alpha} + \frac{\Delta\rho}{\rho}), \quad (5)$$

and

$$R_s \cong \frac{1}{2}(\frac{\Delta\beta}{\beta} + \frac{\Delta\rho}{\rho}), \quad (6)$$

equation (4) becomes

$$R(\theta) = R_p + (R_p - 2R_s)\sin^2\theta . \quad (7)$$

From the equation above we can get

$$R_s = (R_p - G)/2, \quad (8)$$

where G=Rp-2Rs.

This is the AVO attribute equation for estimating the shear wave reflectivity. Given the AVO intercept R_p and AVO gradient G attributes, simply take half of the difference between the two attributes to derive the shear wave reflectivity R_s as described by equation (8).

Shuey's Approximation

Shuey(1985) published a closed form approximation of the Zoeppritz equations which involved α, ρ and σ (Poisson's ratio)

$$R(\theta) = R_p + [R_p A_0 + \frac{\Delta\sigma}{(1-\sigma)^2}]\sin^2\theta + \frac{\Delta\alpha}{2\alpha}(\tan^2\theta - \sin^2\theta), \quad (9)$$

where $\sigma = (\sigma_1 + \sigma_2)/2$, $\Delta\sigma = \sigma_1 + \sigma_2$, $A_0 = B - 2(1+B)\frac{1-2\sigma}{1-\sigma}$, and

$B = \frac{\Delta\alpha/\alpha}{\Delta\alpha/\alpha + \Delta\rho/\rho}$.

With various assumptions, we can simplify the equation (9) as

$$R(\theta) = R_p + G\sin^2\theta \cdot \tag{10}$$

This equation is linear if we plot R as a function of $\sin^2\theta$. We will then perform a linear regression analysis on the seismic amplitudes to estimate intercept R_p, and gradient G. Before performing the linear regression, we must transform our data from constant offset form to constant angle form.

The Smith and Gidlow Approximation

Smith and Gidlow(1987) gave another approximation based on the Aki and Richards equation. They first rearranged equation (3) to get

$$R(\theta) = [\frac{1}{2}(\frac{\Delta\alpha}{\alpha} + \frac{\Delta\rho}{\rho})] - 2\frac{\beta^2}{\alpha^2}[2\frac{\Delta\beta}{\beta} + \frac{\Delta\rho}{\rho}]\sin^2\theta + \frac{1}{2}\frac{\Delta\alpha}{\alpha}\tan^2\theta . \tag{11}$$

And then they simplified equation (11) by removing the dependence on density by using Gardner's relationship

$$\rho = a\alpha^{1/4} . \tag{12}$$

This can be differentiated to give

$$\frac{\Delta\rho}{\rho} = \frac{1}{4}\frac{\Delta\alpha}{\alpha} . \tag{13}$$

Substituting equation (13) into equation (11) gives

$$R(\theta) = c\frac{\Delta\alpha}{\alpha} + d\frac{\Delta\beta}{\beta} , \tag{14}$$

where $c = \frac{5}{8} - \frac{1}{2}\frac{\beta^2}{\alpha^2}\sin^2\theta + \tan^2\theta$ and $d = -4\frac{\beta^2}{\alpha^2}\sin^2\theta$.

Using this equation we can estimate $\Delta\alpha/\alpha$ and $\Delta\beta/\beta$ by using generalized linear inversion (GLI). The GLI solution in matrix form is given by

$$\begin{pmatrix} \sum_i^N a_i^{\,2} & \sum_i^N a_i b_i \\ \sum_i^N a_i b_i & \sum_i^N b_i^{\,2} \end{pmatrix} \begin{pmatrix} \frac{\Delta\alpha}{\alpha} \\ \frac{\Delta\beta}{\beta} \end{pmatrix} = \begin{pmatrix} \sum_i^N a_i X_i \\ \sum_i^N b_i X_i \end{pmatrix} . \tag{15}$$

The two parameters $\Delta\alpha/\alpha$ and $\Delta\beta/\beta$, estimated by using the least squares solution given by equation (15), represent fractional changes in P and S wave velocity. As such, they are related to P and S wave reflectivity, $\Delta I_p / I_p$ and $\Delta I_s / I_s$, respectively.

Smith and Gidlow (1987) also derived two other types of weighted stacks, the "Pseudo- Poisson's ratio reflectivity and the "fluid factor".

Goodway et al.(1998) gave another way to estimate the P wave and S wave fluctuation based on transforming the Aki-Richards equation to the new variables $\Delta I_p / I_p$ and $\Delta I_s / I_s$

$$\begin{aligned} R(\theta) = &[\frac{1}{2}(1+\tan^2\theta)]\frac{\Delta I_p}{I_p} + [4\frac{\beta^2}{\alpha^2}\sin^2\theta]\frac{\Delta I_s}{I_s} \\ &-[\frac{1}{2}\tan^2\theta - 2\frac{\beta^2}{\alpha^2}\sin^2\theta]\frac{\Delta\rho}{\rho} \end{aligned} . \qquad (16)$$

Goodway et al. (1998) implemented a specific form of equation (16) to derive the AVO attributes $\Delta I_p / I_p$ and $\Delta I_s / I_s$. For a specific value of $\alpha/\beta = 2$ and small angles of incidence for which $\tan\theta \approx \sin\theta$, the third term in equation (16) vanishes and equation (16) takes the form

$$R(\theta) = (1+\tan^2\theta)R_p - (2\sin^2\theta)R_s . \qquad (17)$$

Following the estimation of the P wave and S wave fluctuation by using the generalized linear inversion (GLI) given by equation (15), the P wave and S wave impedance can be computed by integration.

In addition, Goodway et al. (1998) estimated two additional AVO attributes in terms of Lame's constant scaled by density- $\lambda\rho$ and $\mu\rho$

$$\begin{aligned} \lambda\rho &= I^2{}_p - 2I^2{}_s \\ \mu\rho &= I^2{}_s \end{aligned} . \qquad (18)$$

Comparison of the Approximations of Zoeppritz's Equation

There are numerous expressions for the linear approximation of Zoeppritz's equation, each with different emphasis. While Bortfeld (1961) emphasized the fluid and rigidity terms which provided insight when interpreting fluid-substitution problems, Aki and Richard's equation emphasized the contribution of variations in the P- and S- wave velocities and density. Shuey, after learning about the contributions of Koefoed and the amplitude dependence on Poisson's ratio, decided to cast Aki and Richards's equation in terms of Poisson's ratio. One of the Shuey's main contributions is that he identified how various rock properties can be associated with near, mid, and far angle ranges. On the right side of Shuey's equation, the first term is the normal-incident reflectivity and this is constant across all incident angles. The second term does not start to contribute significantly until incident angles of 15 degree or greater are reached. The third term, Shuey argued, is insignificant and can be ignored if the incident-angle range is less than 30 degrees.

Both the first and second term in Shuey's equation contain the normal-incident reflection coefficient. Verm and Hilterman (1995) rearranged Shuey's equation to emphasize the rock property dependence on incident angle:

$$R(\theta) = \frac{1}{2}\left(\frac{\Delta\alpha}{\alpha} + \frac{\Delta\rho}{\rho}\right)\left(1 - \frac{4\beta^2}{\alpha^2}\sin^2\theta\right) + \frac{\Delta\sigma}{(1-\sigma)^2}\sin^2\theta + \frac{\Delta\alpha}{2\alpha}(\tan^2\theta - \frac{4\beta^2}{\alpha^2}\sin^2\theta) \quad (19)$$

With this new arrangement (equation (19)), the near angle response is basically influenced by changes in acoustic impedance; the mid angle response is influenced by variations in Poisson's ratio, and the far angle, by variation in P-wave velocity.

AVO Classification

Rutherford and Williams's classification of the reflection coefficient curves has become the industry standard and it is associated respectively with 1970s classification of bright spot, phase reversal, and dim out. The classification was developed for reflections from hydrocarbon saturated formations. According to Rutherford and Williams's classification, the slope of the reflection coefficient curve is negative for all classes. The reflection amplitude decreases with the angle of incidence. However, the absolute amplitude can increase with angle of incidence as depicted for Class 2 and 3 AVO gas saturated anomalies. Castagna et al. (1998) found that certain Class 3 gas saturated anomalies can have slowly decreasing amplitudes with offset. These were named Class 4 AVO anomalies. However, the main diagnostic feature for the Class 4 anomalies is still the large amplitude associated with the hydrocarbons.

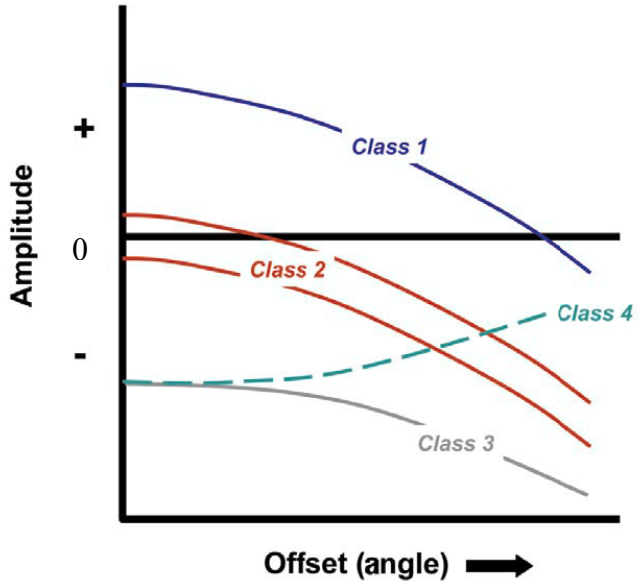

FIG. 2. Classification of AVO Responses Class 1, Class 2, Class 3, and Class 4. (Rutherford and Williams, 1989).

Class 1 (Dim out) anomalies have the following properties:

- Amplitude decreases with increasing angle, and may reverse phase on the far angle stack
- Amplitude on the full stack is smaller for the hydrocarbon zone than for an equivalent wet saturated zone.
- Wavelet character is peak-trough on near angle stack
- Wavelet character may or may not be peak-trough on the far angle stack.

Class 2 (Phase reversal) anomalies have the following properties:

- There is little indication of the gas sand on the near angle stack.
- The gas sand event increases amplitude with increasing angle. This attribute is more pronounced than anticipated because of the amplitude decrease of the shale-upon-shale reflections.
- The gas sand event may or may not be evident on the full stack, depending on the far angle amplitude contribution to the stack.
- Wavelet character on the stack may or may not be trough-peak for a hydrocarbon charged thin bed.
- Wavelet character is trough-peak on the far angle stack.
- Inferences about lithology are contained in the amplitude variation with incident angle.
- AVO alone, unless carefully calibrated, cannot unambiguously distinguish a clean wet sand from a gas sand, because both have similar (increasing) behavior with offset.

Class 3 (Bright spot) anomalies have the following properties:

- Hydrocarbon zones are bright on the stack section and on all angle limited stacks.
- The hydrocarbon reflection amplitude, with respect to the background reflection amplitude, is constant or increases slightly with incident angle range. Even though the amplitude of the hydrocarbon event can decrease with angle, as suggested for the Class 4 AVO anomalies, the surrounding shale-upon-shale reflections normally decrease in amplitude with angle at a faster rate.
- Wavelet character is trough-peak on all angle stacks. This assumes that the dominant phase of the seismic wavelet is zero and the reservoir is below tuning thickness.

- Hydrocarbon prediction is possible from the stack section.

SEISMIC DATA PROCESSING FOR AVO/AVA ANALYSIS

AVO processing and analysis is intended to provide additional rock properties and reservoir properties from seismic data beyond structural imaging. AVO analysis mainly relies on fitting gradients to amplitude observations over a range of offsets. In order that the resulting gradient fits be considered reliable, all steps in the data processing sequence must accurately preserve the natural amplitude variations related to lithology and fluid content. Velocities must be accurate and scaling must maintain relative amplitudes. Interference due to noise and multiples or side effects related to their attenuation must be carefully monitored. The amplitude bias introduced by various algorithms should be taken into account.

Yilmaz (2001) addressed the detailed processing sequence in his book. There are three important aspects of a processing sequence tailored for AVO analysis.

- The relative amplitudes of the seismic data must be preserved throughout the analysis in order to recognize amplitude variation with offset.

- The processing sequence must retain the broadest possible signal band in the data with a flat spectrum within the passband.

- Prestack amplitude inversion to derive the AVO attributes must be applied to common reflection point (CRP) gathers.

Noise Attenuation

During the AVO processing there are various types of noise that distort the true amplitudes of the seismic data. These noises have to be removed by different noise suppression processes. Dey-Sarkar and Svatek (1993) defined three basic types of noise that distort the amplitudes in the prestack domain. Type I noise is associated with source generated noise, multiples, surface consistent effects. Fourier transform techniques and surface-consistent computation can be used to remove these effects. Type II noise is generally associated with instrumentation or cultural noise during data acquisition. Type III noises are entirely due to wave propagation effects in a visco-elastic medium.

The approach proposed by Dey-Sarkar and Svatek (1993) is to calibrate the amplitudes using some statistical algorithms. After removing Type I and Type II noises from the prestack data, there are mainly two components of the amplitude left. The first component is associated with the amplitude variation due to Type III noise. The second component is associated with the reflection coefficient variation with offset. Dey-Sarkar and Svatek (1993) estimate the first component (Type III noise) from a window of events above the target event. The RMS amplitudes are computed for each offset and an exponential decay function is fitted through the data points. The coefficient of this decay function is the amplitude correction factor for the event. The coefficient is spatially averaged to obtain a smoothly varying function. The advantages of this technique are, (1)

the robustness, (2) no subsurface parameters are assumed, and (3) no distortion is produced in the data because of the slowly varying function.

Xu and Bancroft (1997) applied this method to the multi-component data acquired from Blackfoot, Alberta (see Figure 3).

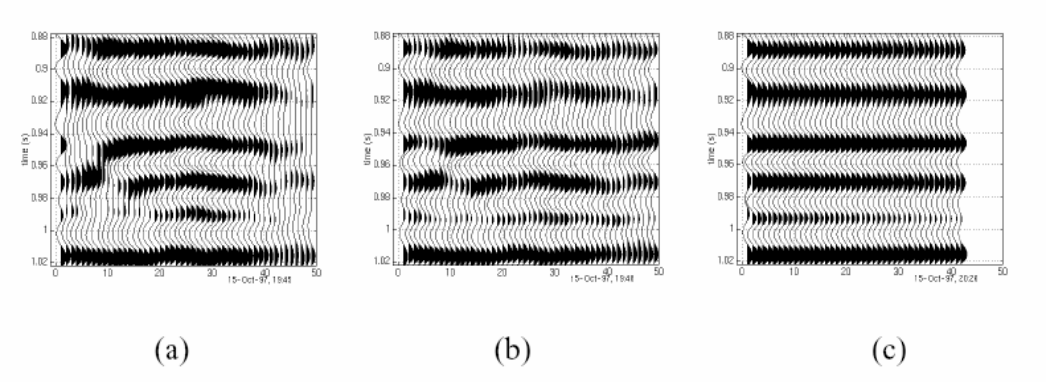

FIG. 3. (a) The gather before amplitude calibration. (b) The gather after amplitude calibration. (c) The synthetic gather. (Xu and Bancroft, 1997).

True Amplitude Radon Transform

When the data are severely contaminated by multiples, the Radon transform is a popular tool for regularization and preprocessing of seismic data prior to migration, AVO analysis and stratigraphic interpretation.

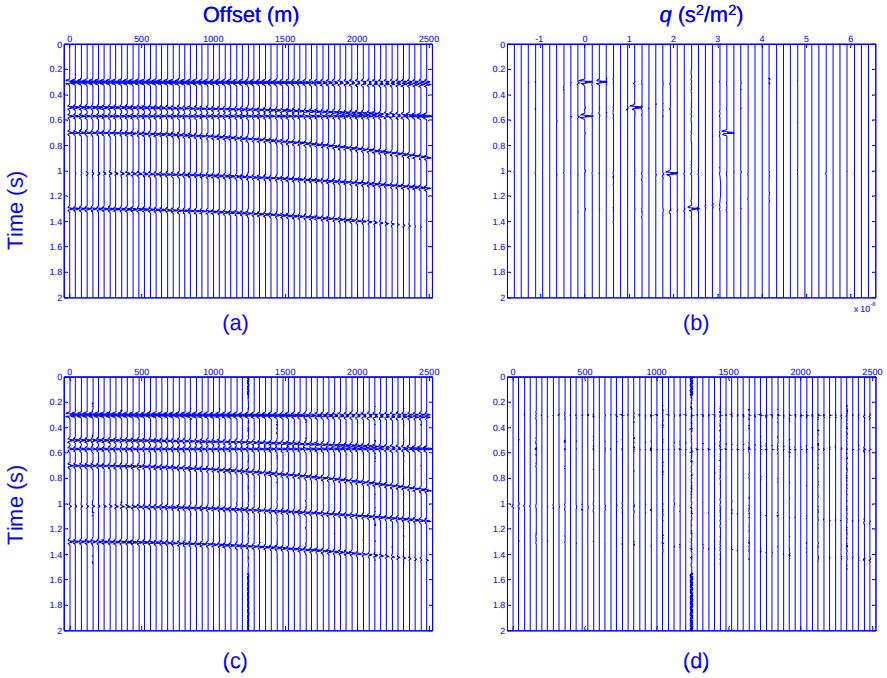

FIG. 4. Results of the improved semblance-weighted Radon method: (a) The model; (b) The Radon panel; (c) The reconstructed gather; and (d) The residual gather. (Cao, Bancroft, 2004).

We often use the Radon transform to suppress ground roll, coherent noise, and multiples. Suppression of coherent noise greatly facilitates prestack migration velocity analysis. However, for AVO analysis, it is most important to make sure that any removal of noise does not degrade the signal component of the reflections.

Nurrul (1999) addressed how to remove the multiples and preserve the true amplitude at the same time. A weighting approach was applied to the least squares Radon transforms to preserve the amplitude.

Cao and Bancroft (2004) worked on the parabolic semblance-weighted Radon transform with a Gauss-Seidel iterative method in the time domain. This approach can enhance energy clusters along those trajectories which fit seismic events well in the seismic dataset and weaken energy along those trajectories which badly fit seismic events. Applied in the Gauss-Seidel sense, the semblance-weighted Radon approach produces moderately high resolution results and the amplitude was well preserved (see Figure 4).

True Amplitude DMO

A true amplitude DMO approach for improving AVO analysis was demonstrated by Ramos (1999). True-amplitude DMO can reduce the amplitude mix caused by the smearing and the mis-positioning of reflection points. The main advantage of true amplitude DMO compared to more traditional methods lies in its ability to perform a better compensation of geometrical spreading losses with offset. He showed that the application of true amplitude DMO on a real dataset with a real AVO anomaly resulted in better estimation of more reliable amplitude, AVO gradient, better delineation and enhancement of AVO anomalies (Figure 5).

For F-K DMO case, we can notice that there is a considerably smaller scatter of the amplitudes around the background trend. This smaller scatter leads to a poor gradient estimation, especially for the long offsets and steeply dipping events. The crossplots for the true amplitude DMO case shows a significantly larger scatter and a better separation of the anomalous values in the first and third quadrants, due to more accurate geometrical spreading compensation for amplitudes at far offsets (Ramos et al., 1999).

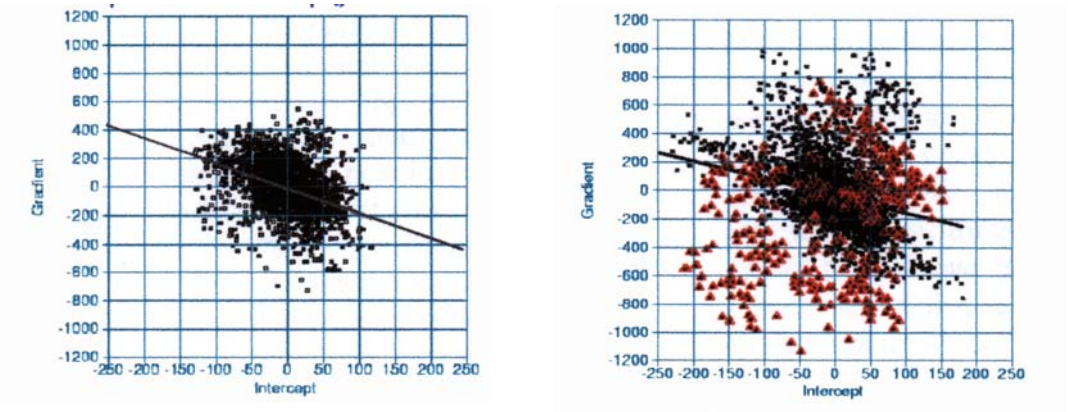

FIG. 5. Cross plot gradient versus intercept for the seismic data processed with f-k DMO (left) and true-amplitude DMO (right). (Ramos, 1999).

True Amplitude Migration

During the initial era of AVO analysis, one performed the analysis mainly on common-midpoint (CMP) gathers of the unmigrated data. But for steeply dipping reflectors and more complicated structure, the result of the AVO analysis often lacks accuracy due to the effects of CMP smearing. It is worth analyzing AVO in common-reflection-point (CRP) gathers after prestack migration.

Generally speaking, Kirchhoff migration can produce both reflection coefficients and reflection angles at image locations, making it ideal for AVO analysis in areas of moderate structural complexity. A lot of published examples have shown accurate amplitudes after Kirchhoff migration. Factors affecting AVO analysis of Prestack migration gather were addressed by Zhang (2002). Sparsity of azimuth sampling, incorrect choice of migration weights and anti-aliasing filters can affect the AVO signatures.

Tydel (1999) investigated the effect of the various true amplitude Kirchhoff migration methods on AVO/AVA response. In his study, simple CMP AVO processing, true amplitude PreSDM and the true amplitude MZO (Migration to Zero Offset) algorithm was applied to an ensemble of individual common offset sections.

His main conclusion is that both true amplitude PreSDM and MZO are very well suited for AVO/AVA analysis. The true amplitude PreSDM amplitude did not suffer more from inaccuracies in the migration velocity than MZO amplitude. The angle transform was more sensitive to migration velocity than reflection coefficients. PreSDM has better noise reduction. Due to having no amplitude preserving antialiasing filter, MZO will be more severely affected than PreSDM when applied to field data with insufficient trace spacing.

Yilmaz (2001) pointed out that the phase shift method should be used for AVO analysis, because differencing approximations to differential operators are used in finite difference migrations. The usual implementation of Kirchhoff migration does not include all the terms of the integral solution to the scalar wave equation. As such, the missing terms can influence the amplitude and phase accuracy of the resulting migrated data.

AVO Processing Sequence

The success of the AVO technique relies not only on the algorithm but also the processing sequence. However, amplitude preservation throughout the processing sequence can be difficult to achieve. When seismic anomalies are extremely large, AVO effects stand out, and sometimes the bias introduced by processing algorithms may not be sensed at all. Small amplitude anomalies, often associated with the presence of liquid hydrocarbons, normally show small expression, which can be completely lost or destroyed by unsatisfactory data preconditioning. Allen and Peddy (1993) showed an example where two of three processors failed to identify a subtle AVO anomaly at a gas discovery.

The goal of true amplitude processing is to obtain reliable data for AVO analysis. The biggest issue in AVO processing combines algorithms and processing parameters in a

balanced way, creating the minimal amount of amplitude bias. Ramos (2001) pointed out that the success of AVO technique relies considerably upon the processing sequence employed, especially in the presence of strong multiples and reverberations. His study also demonstrated that AVO should be used with caution as an exploration tool, but it can be used more safely in areas where the calibration processing is possible.

AVO INVERSION

Smith and Gidlow (1987) developed the ground-breaking methodology, now commonly used for transforming NMO corrected gathers into estimates of rock properties, by the use of weighted stacking. The method calculates AVO fluctuation by least squares fitting a curve that approximates the Zoeppritz equation to a crossplot of reflection amplitudes as a function of reflection angle for a given CMP. Inversion is performed using either a 2-term or 3-term approximation to the Zoeppritz equation. The most commonly used approximations are those derived by Shuey (1985) for 2-term inversion, and Aki and Richards (1980) for 3-term inversions.

A 2-term inversion effectively gives us just two AVO attributes, either AVO Intercept and AVO Gradient or Normal Incidence Reflectivity and Poisson Reflectivity. While the 2-term inversion is growing in popularity through the acceptance of AVO crossplots as an interpretation tool, it is often overlooked that the Shuey approximation is invalid beyond about 30 degrees angle of incidence. A full 3-term inversion will solve for P-wave reflectivity, S-wave reflectivity and density reflectivity and will generally honour the Zoeppritz response accurately to about 50 degrees angle of incidence, which is common in today's long-offset acquisition geometries. These attributes may then be combined or inverted (through a process of Elastic Inversion) to calculate more indicative hydrocarbon indicators such as Fluid Factor, Poisson Reflectivity or the Lamé parameters of Lambda-Rho ($\lambda\rho$) and Mu-Rho ($\mu\rho$) corresponding to the product of density and the elastic properties of incompressibility and rigidity respectively.

Three terms inversion of P-P data

The idea of three terms least-squares inversion of P-P data is usually credited to Smith and Gidlow (1987) who showed that the Aki and Richards approximation for R_{pp} can be inverted by least squares to estimate the fluctuation $\Delta\alpha/\alpha$, $\Delta\beta/\beta$ and $\Delta\rho/\rho$,. In their method, P-P reflection data are assumed to provide estimates of R_{pp} over a range of source-receiver offsets. Thus, for each incident angle θ, an equation can be written like

$$R_{pp} = a\frac{\Delta\alpha}{\alpha} + b\frac{\Delta\rho}{\rho} + c\frac{\Delta\beta}{\beta}, \qquad (20)$$

where $a = 1/(2\cos^2\theta) = (1+\tan^2\theta)/2$, $b = 0.5 - [(2\beta^2/\alpha^2)\sin^2\theta]$,
$c = -(4\beta^2/\alpha^2\sin^2\theta)$, $\alpha = (\alpha_1+\alpha_2)/2$, $\beta = (\beta_1+\beta_2)/2$, $\rho = (\rho_1+\rho_2)/2$,

$\Delta\alpha = \alpha_2 - \alpha_1$, $\Delta\beta = \beta_2 - \beta_1$, $\Delta\rho = \rho_2 - \rho_1$, $\theta = (\theta_i + \theta_t)/2$, and $\theta_t = \arcsin[(\alpha_2/\alpha_1)\sin\theta_i]$.

We note the explicit dependence on the incidence angle θ. Then, considering all available offsets, a matrix equation can be constructed

$$\begin{bmatrix} R_{pp}(\theta_1) \\ R_{pp}(\theta_2) \\ \vdots \\ R_{pp}(\theta_n) \end{bmatrix} = \begin{bmatrix} a(\theta_1) & b(\theta_1) & c(\theta_1) \\ a(\theta_2) & b(\theta_2) & c(\theta_2) \\ \vdots & \vdots & \vdots \\ a(\theta_n) & b(\theta_n) & c(\theta_n) \end{bmatrix} \begin{bmatrix} \Delta\alpha/\alpha \\ \Delta\beta/\beta \\ \Delta\rho/\rho \end{bmatrix}. \tag{21}$$

The left side of this equation is a column vector representing the amplitudes of a particular P-P reflection as a function of offset. The n×3matrix on the right contains the coefficients a, b, c. computed at the appropriate incidence angle for each offset. This matrix is approximately known if a background velocity model is available to raytrace in order to obtain the incidence angles. Finally, the column vector on the right contains the unknown fluctuation to be estimated. If there are more than three offsets, there are more equations than unknowns and least-squares inversion is appropriate. Writing this equation symbolically as $R=CF$, its least-square inverse is $F=AR$, where $A = \left(C^T C\right)^{-1} C^T$. Smith and Gidlow were able to calculate the entries in the matrix A analytically and showed that the algorithm $F=AR$ is just a weighted stack. That is, F can be estimated, in principle, by an equation of the form

$$F_\alpha = \sum_{k,offset} a(\theta_k) R_{pp}(\theta_k). \tag{22}$$

With similar equations, having different weighting functions, for $F_\alpha, F_\beta, F_\rho$. In this equation, the sum is over all available offsets and the weights, $a(\theta_k)$, are known functions of the background velocity and the incidence angle for the k_{th} offset. Usually, it is expected that the overall density effect on R_{pp} is small and this implies that inversion for $F_\alpha, F_\beta, F_\rho$ will be problematic with noisy data.

Smith and Gidlow (1987) suggested using Gardner's relation that $\rho \approx k\alpha^{0.25}$ (k is a constant whose numerical value depends upon the system of units employed) to convert the density dependence into an additional P-wave velocity term. An alternative approach is the approach of Fatti et al. (1994) who reformulated the equations to invert for fluctuation associated with P-wave and S-wave impedances:

$$\begin{aligned} F_I &= \Delta(\rho\alpha)/\rho\alpha \\ F_J &= \Delta(\rho\beta)/\rho\beta \end{aligned}. \tag{23}$$

This avoids the use of Gardner's rule but there is still an independent F_ρ term that must be neglected. Fortunately, the coefficient of this term is generally small.

Other Petrophysical Discrimination

A number of derived attributes may be used to highlight changes in lithology and pore fluid content. Smith and Gidlow (1987) discussed two possibilities, the pseudo- Poisson's ratio reflectivity and the fluid factor reflectivity. These attributes can be directly calculated from estimates of $\Delta\alpha/\alpha$, $\Delta\beta/\beta$, or $\Delta I/I$ and $\Delta J/J$. The pseudo- Poisson's ratio reflectivity or fractional *Vp/Vs* ratio is given by

$$\frac{\Delta q}{q} \equiv \frac{\Delta(\alpha/\beta)}{\alpha/\beta} = \frac{\Delta(I/J)}{I/J} = \frac{\Delta\alpha}{\alpha} - \frac{\Delta\beta}{\beta} = \frac{\Delta I}{I} - \frac{\Delta J}{J}. \qquad (24)$$

Equation (24) allows the calculation of normalized changes in *Vp/Vs* ratios, which can be directly correlated to lithological and/or pore fluid content changes.

The fluid factor reflectivity is highly dependent upon local geology and measures deviations from the 'mudrock line' of Castagna et al. (1985). The fluid factor is generally considered accurate for water saturated clastic sedimentary rocks, but deviates significantly for gas-saturated clastics, carbonates and igneous rocks. The 'mudrock line' is an empirical relation between α and β thought to typify shales. It is given by Castagna et al. (1985) as

$$\alpha \approx a + b\beta = 1360 + 1.16\beta. \qquad (25)$$

For a given locality, *a* and *b* should be derived from well-constrained, dipole sonic log information. The derivation of the 'fluid factor reflectivity' from equation (25) is straightforward, if we let *g* equal the deviation from the mudrock line

$$g = \alpha - a - b\beta. \qquad (26)$$

Note the parameter *g* will be zero for exact adherence to the 'mudrock line' of equation (26). Now, the finite difference of equation (26),

$$\Delta g = \Delta\alpha - b\Delta\beta. \qquad (27)$$

And define the fluid factor Δf ,

$$\Delta f = \frac{\Delta g}{\alpha} = \left(\frac{\Delta\alpha}{\alpha} - b\frac{\Delta\beta}{\alpha}\right) = \left(\frac{\Delta\alpha}{\alpha} - b\frac{\beta}{\alpha}\frac{\Delta\beta}{\beta}\right) = \left[\frac{\Delta I}{I} - b\frac{\beta}{\alpha}\frac{\Delta J}{J} - \frac{\Delta\rho}{\rho}\left(1 - b\frac{\beta}{\alpha}\right)\right]. \qquad (28)$$

Therefore any deviations from the fluid factor indicate a deviation from the 'mudrock line' (equation 27). The potentially awkward step of calculating estimates of $\Delta\rho/\rho$ in equation 28 above generally limits the use of the fluid factor reflectivity when inverting for compressional and shear impedance.

Several authors have alluded to the need for greater physical insight into the underlying physical rock properties contained in compressional and shear velocities (Wright 1984, Thomsen, 1990, Castagna et al., 1993). From these observations it is sensible to conclude the possible utility of extracting rigidity and shear modulus rock properties directly from AVO analysis. Stewart (1995) provides a method for directly

extracting elastic modulus parameters from the Zoeppritz equation approximations of Aki and Richards (1980). Stewart further advised that λ/μ may be used to highlight pore-fluid contrasts rather than changes in lithology. This concept was successfully tested by Goodway et al. (1997) to show the potential of improved petrophysical discrimination using Lame parameters $\lambda\rho, \mu\rho, \lambda/\mu$. This method is summarized by the following set of equations:

$$\frac{\Delta(\lambda\rho)}{\lambda\rho} = \frac{2}{\alpha^2 - 2\beta^2}\left(\alpha^2 \frac{\Delta I}{I} - 2\beta^2 \frac{\Delta J}{J}\right), \tag{29}$$

$$\frac{\Delta(\mu\rho)}{\mu\rho} = 2\frac{\Delta J}{J}, \tag{30}$$

$$\frac{\Delta(\lambda/\mu)}{\lambda/\mu} = \frac{2}{\alpha^2 - 2\beta^2}\left(\frac{\Delta I}{I} - \frac{\Delta J}{J}\right) = \frac{2}{\alpha^2 - 2\beta^2}\frac{\Delta q}{q}. \tag{31}$$

For completeness, the fractional Poisson ratio and bulk modulus ratios can also be defined,

$$\frac{\Delta\sigma}{\sigma} = \frac{2\alpha^2\beta^2}{(\alpha^2 - \beta^2)(\alpha^2 - 2\beta^2)}\left(\frac{\Delta I}{I} - \frac{\Delta J}{J}\right) = \frac{2\alpha^2\beta^2}{(\alpha^2 - \beta^2)(\alpha^2 - 2\beta^2)}\frac{\Delta q}{q}, \tag{32}$$

$$\frac{\Delta(\kappa\rho)}{\kappa\rho} = \frac{2}{(\alpha^2 - 4/3\beta^2)}\left(\alpha^2 \frac{\Delta I}{I} - \frac{4}{3}\beta^2 \frac{\Delta J}{J}\right). \tag{33}$$

Note equations 29, 30, 31, 32 and 33 represent weighted functions of the previously derived estimates of $\Delta I/I$ and $\Delta J/J$. In practice, the smoothed background model provides the weights.

Joint AVO Inversion of PP and PS Data

Stewart (1990) derived the extension of the Smith-Gidlow approach that uses both PP and PS reflections to constrain the reflectivity $\Delta\alpha/\alpha$, $\Delta\beta/\beta$ and $\Delta\rho/\rho$. Larsen et al. (1998) and Larsen (1999) presented a practical implementation of these ideas as applied to the Blackfoot 3C-3D survey. Like Smith and Gidlow (1987), Stewart (1990) developed exact analytic forms for the stacking weights of both PP and PS data. The algebraic expressions for these weights are too complex to present here. In essence, the fluctuation are estimated by equations of the form

$$\frac{\Delta\alpha}{\alpha} = \sum_{k,offset} a(\theta_k) R_{pp}(\theta_k) + \sum_{k,offset} b(\theta_k) R_{ps}(\theta_k). \tag{34}$$

Where θ_k is the P-wave incidence angle for the kth offset, $a(\theta_k)$ are the stacking weights for the PP reflection data, and $b(\theta_k)$ are the weights for the PS reflection data. Similar equations, with different weights, will estimate $\Delta\beta/\beta, \Delta\rho/\rho$. The weights for

the PP reflection data, $a(\theta_k)$, in this expression are generally quite different from the analogous weights in the inversion using PP data alone.

As with the PP case, it is often preferable to bypass the estimation of $\Delta\rho/\rho$. Larsen (1999) shows that either the Smith-Gidlow approach using Gardner's rule or the Fatti approach of estimating impedance is possible. In the latter case, there is again $\Delta\rho/\rho$ term that must be neglected. Interestingly, the possibility of a true three-parameter inversion for $\Delta\alpha/\alpha$, $\Delta\beta/\beta$, $\Delta\rho/\rho$, is much more feasible with PP and PS data.

Margrave and Stewart (2001) used the PP and PS joint inversion and documented its performance, in comparison with PP data alone, using the 3C-3D survey at Blackfoot field. Like the PP method, the joint method is implemented as a weighted stack but with different weights and twice the statistical leverage. The joint method gives markedly superior estimates of the P-wave and S-wave impedance fluctuation, but only moderately better estimates of the pseudo-Poisson's ratio.

Other Non-linear Inversion Methods

In the previous section the inversion methods discussed are linear inversion methods. For linear inversion, it is not a global optimization algorithm. This means that the possibility exists for the algorithm to become "trapped" in a local minimum. However, a non-linear inversion algorithm can skip the local minimum to find the global minimum. The most commonly used non-linear inversion algorithms are the genetic, artificial neural network and Monte Carlo algorithms.

Mogensen (2000) applied artificial neural network solutions to estimate P-wave, S-wave velocity, and Poisson's ratio from simulated seismic data.

Mallick (2001) successfully applied prestack genetic inversion in continuous prestack inversion, hybrid inversion, and geo-hazard studies such as pore pressure prediction and shallow water flow (SWF) prediction.

SUMMARY

Approximately 30 research papers on AVO, which include the principles of AVO, seismic data processing and inversion for AVO analysis were reviewed in this study. This review is not intended to be exhaustive but should give the reader a good introduction to the development of the theories and techniques of AVO processing and inversion. The main trend in the AVO development is shifting from more theoretical studies to more applications, from P-wave seismic data to multicomponent seismic data. This trend results in successful solutions to more and more challenging problems encountered by scientists in petroleum exploration.

ACKNOWLEDGEMENTS

We would like to thank the CREWES sponsors for their financial assistance in this project and J. Wong for helping edit this paper.

REFERENCES

Aki, K., and Richards, P.G., 1980, Quantitative seismology: Theory and methods: W. H. Freeman and Co.

Allen, J.L. and Peddy, C.P., 1993. Amplitude Variation with Offset Gulf Coast Case Studies. Society of Exploration Geophysicists, Tulsa, OK., 120 pp.

Bortfeld, R., 1961, Approximation to the reflection and transmission coefficients of plane longitudinal and transverse waves: Geophys. Prosp., **9**, 485-503.

Castagna, J.P. and Backus, M.M., 1993, AVO analysis-tutorial and review, in Castagna, J. and Backus, M.M., eds, Offset-dependent reflectivity . Theory and practice of AVO analysis: Soc. Expl. Geophysics, 3-37.

Castagna, J.P. and Swan, H.W., 1998, Principles of AVO crossplotting: The Leading Edge, 16, 337-342.

Chiburis, E.F., 1984, Analysis of amplitude versus offset to detect gas-oil contacts in Arabia Gulf: 54th Ann. Internat. Mtg., Soc. Expl. Geophys., Expanded Abstracts, 669-670.

Dey-Sarkar, S. K., and Svatek, S. V., Prestack analysis – An integrated approach for seismic interpretation in Clastic basins in Castagna, J. P., and Backus, M. M., Eds., Offsetdependent reflectivity--Theory and practice of AVO analysis, Soc. Expl. Geophys., 57-77.

Gary F. Margrave and Robert R. Stewart, Joint P-P and P-S seismic inversion, CREWES, University of Calgary.

Goodway, B., Chen, T., and Downton, J., 1998, Improved AVO fluid detection and lithology discrimination using Lamé petrophysical parameters; .λρ ., .μρ ., & .λ μ fluid stack., from P and S inversions: 67th Ann. Internat. Mtg., Soc. Expl. Geophys., Expanded Abstracts, 183-186.

John C. Bancroft and Zhihong Cao, A comparison of CMP and EO gathers for multiple-attenuation, 2004 CSEG convention.

Knott, C.G., 1899, Reflexion and refraction of elastic waves with seismological applications: Phil. Mag., **48**, 64-97.

Koefoed, O., 1955, On the effect of Poisson.s ratios of rock strata on the reflection coefficients of plane waves: Geophys. Prosp., **3**, 381-387.

Larsen, J.A., Margrave, G.F., and Lu, H., 1999, AVO analysis by simultaneous P-P and P-S weighted stacking applied to 3C-3D seismic data: 69th Ann. Internat. Mtg., Soc. Expl. Geophys., Expanded Abstracts, 721-723.

Lines, L.R. and Treitel, S., 1984, Tutorial: A review of least-squares inversion and its application to geophysical problems: Geophys. Prosp., **32**, 159-186.

M. M. Nurul Kabir and Kurt J. Marfurt, 1999, Toward true amplitude multiple removal, The Leading Edge, **18**, pp. 66-73 (January 1999).

Mallick, S. and Frazer, L.N., 1991, Reflection/transmission coefficients and azimuthal isotropy in marine studies: Geophys. J. Internat., **105**, 241-252.

Martin Tygel, Lucio T. Santos, Joerg Schleicher, and Peter Hubral: Kirchhoff imaging as a tool for AVO/AVA analysis The Leading Edge 1999, **18**,: 940-945.

Ostrander, W.J., 1982, Plane-wave reflection coefficients for gas sands at nonnormal angles of incidence: Geophysics, **49**, 1637-1648.

Ostrander, W.J., 1984, Plane-wave reflection coefficients for gas sands at nonnormal angles of incidence: Geophysics, **49**, 1637-1648.

Ramos, A.C.B., Oliveira, A.S., and Tygel, M., 1999, The impact of true amplitude DMO on amplitude versus offset: 69th Ann. Internat. Mtg., Soc. Expl. Geophys., Expanded Abstracts, 832-835.

Richards, P.G. and Frasier, C.W., 1976, Scattering of elastic waves from depth-dependent inhomogeneties: Geophysics, **41**, 441-458.

Shuey, R.T., 1985. A simplification of the Zoeppritz equations: Geophysics, **50**, p. 609-614.

Gelfand, V., et al, 1986: "Seismic Lithologic Modeling of Amplitude-versus-offset Data", Proceedings of the 56th Annual Meeting of the SEG, Nov. 2-6, 1986, p. 334-336

Smith, G.C. and Gidlow, P.M., 1987, Weighted stacking for rock property estimation and detection of gas: Geophys. Prosp., **35**, 993-1014.

Stewart R.R., Zhang, Q., and Guthoff, F., 1995, Relationships among elastic-wave values (Rpp, Rps, Rss, Vp, Vs, ρ , σ , κ) CREWES Report **7**, 10, 1-9.

Stewart, R.R., 1990, Joint P and P-SV inversion, CREWES Research Report, **2**, 1990.

Thomsen, L., 1993, Weak anisotropic reflections, in Castagna, J. and Backus, M., Eds, Offset dependent reflectivity . Theory and practice of AVO analysis: Soc. Expl. Geophys., 103-114.

Verm, R. and Hilterman, F., 1995, Lithology color-coded seismic sections: The calibration of AVO crossplotting to rock properties: The Leading Edge, **14**, 847-853.

Wright, J., 1997, The effects of transverse isotropy on reflection amplitude versus offset: Geophysics, **52**, 564-567.

Yong Xu and John C. Bancroft, 1997, Joint AVO analysis of PP and PS seismic data, CREWES Research Report, **9**.

Zoeppritz, K., 1919, Erdbebenwellen VIIIB, On the reflection and propagation of seismic waves: Göttinger Nachrichten, **I**, 66-84.

Yilmaz, O., 2001, Seismic data analysis: Society of Exploration.